Accumulation variation in eastern Kemp Land, Antarctica

IAN D. GOODWIN,

School of Earth Sciences, University of Melbourne, Parkville, Victoria 3052, Australia

MARTIN HIGHAM, IAN ALLISON,

Antarctic Cooperative Research Centre, Box 252C, Hobart, Tasmania 7001, Australia and Australian Antarctic Division

REN JAIWEN

Lanzhou Institute of Glaciology and Geocryology, Chinese Academy of Sciences, Lanzhou 730000, China

ABSTRACT. The spatial pattern of accumulation rate for eastern Kemp Land in the elevation range 1850–2700 m is presented together with observations of the physical parameters of snow temperature, average microwave emissivity (19 GHz, H polarization), distribution of depth hoar and firn-crystal diameter. The broad accumulation pattern in the region was found to be significantly low when compared to other coastal areas of East Antarctica such as Wilkes Land. The low accumulation regime is attributed to low atmospheric moisture transport and low penetration of synoptic cyclonic systems on to the coastal slopes. In the absence of high coastal precipitation, the accumulation rate is determined predominantly by surface snow-redistribution processes. Attempts to determine accumulation-rate time series using visible layer, $\delta^{18}O$ isotope and electrical conductivity stratigraphies were unsuccessful due to the relatively low coastal accumulation rates (less than $280 \, \text{kg m}^{-2} \text{a}^{-1}$) and the complex modification of precipitation by redistribution processes. $\delta^{18}O$ variations of seemingly cyclic nature observed throughout the cores were interpreted as a product of the snow-dune building and erosion processes, together with general redistribution of snows by the surface wind field, under the influence of mesoscale topographic roughness.

INTRODUCTION

Eastern Kemp Land is located on the western slopes of the Lambert Glacier basin (Fig. 1). The continental-wide accumulation-rate distributions published by Drewry and Morris (1992) and Giovinetto and Bull (1987) indicate that coastal accumulation rates reach their lowest values in the Kemp Land region, between 50° and 60° E. This region of low coastal accumulation rates contrasts with the higher coastal accumulation-rate pattern in Wilkes Land investigated earlier (Goodwin, 1990, 1991).

As part of the ANARE Lambert Amery Regional Glaciology Experiment (LARGE), spatial accumulation-rate measurements in Kemp Land were made on canes placed every 2 km along the main oversnow traverse route between about 55° and 61° E for the period 1989–92 (Fig. 1). Previous measurements were made along approximately 68°39′ S for the period 1975–78 (Morgan and Jacka, 1981). The elevation range of the accumulation measurements is between 1850 and 2700 m. Shallow firn-core drilling to depths of 15–27 m was carried out at seven locations in an attempt to determine accumulation-rate time series for the region. Three of the drilling sites (LGB00, MGA and E065) were located along the line reported by Morgan and Jacka (1981) and are discussed in this paper. Accumulation-rate time series were also measured between 1983 and 1992 at a grid of 25 canes spaced at 50 m intervals at LGB00. The spatial and temporal accumulation-rate measurements and distributions are discussed together with the dominant surface processes observed throughout the region.

SPATIAL ACCUMULATION DISTRIBUTION

The 10 km mean accumulation-rate measurements (five-cane averages) along the traverse route are shown in Figure 2 for the epoch 1989–92 (although the southernmost 120 km are for 1989–90 only). The accumulation and elevation profiles are plotted against continentality (distance from the coast and moisture source). For comparison, the 10 km mean accumulation-rate measurement for 110° E is also shown in Figure 2 for the same elevation range. The 110° E region is representative of Wilkes Land and the coastal slopes of much of East Antarctica.

For the Kemp Land line, the accumulation-rate pattern displays almost no systematic variation from a mean of approximately $150 \, \text{kg m}^{-2} \text{a}^{-1}$ with either elevation or continentality. Variability along this line is high, with a range of between 80 and $200 \, \text{kg m}^{-2} \text{a}^{-1}$. In contrast, the Wilkes Land profile displays a typically strong gradient of decreasing accumulation with both increasing elevation and continentality. The accumulation in Wilkes Land is approximately twice that of
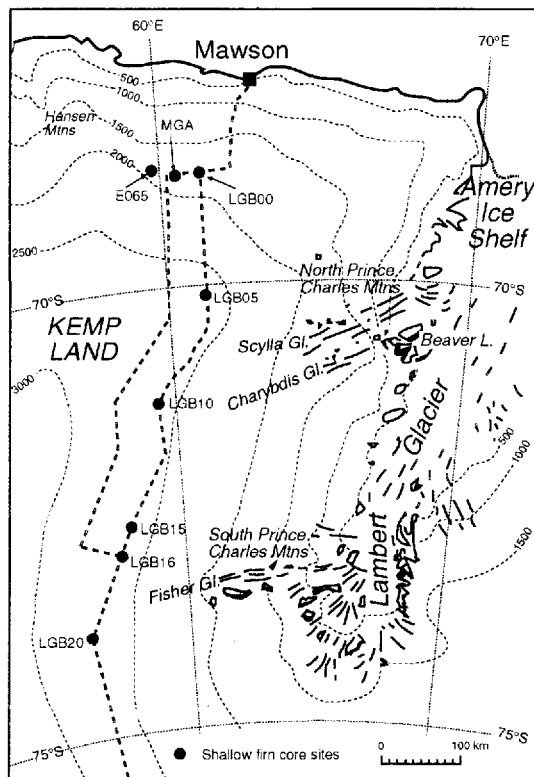
Fig. 1. Location map showing traverse routes and sites of shallow firn cores drilled in 1990–91 and 1992–93. Elevation contours are derived from Drewry (1983) and ANARE traverses.

Kemp Land at 1850 m elevation and approximately the same at 2600 m.

The difference in accumulation rates below 2600 m for the two regions, and the equivalence above 2600 m, is interpreted as being due to the different snow-precipitation mechanisms experienced by the coastal slopes and the interior plateau. Below 2600 m, on the coastal slope of Wilkes Land, the precipitation is controlled by incursions of maritime air masses. However, Bromwich (1988) showed from modelling that the atmospheric

moisture transport in the western Lambert Glacier basin is anomalously low because net air movement is northward, rather than southward or poleward, as for the remainder of East Antarctica. Strong penetration of maritime cyclones across the coastal slopes in Kemp Land is not apparent. In addition, Giovinetto and others (1992) indicated that the coastal slopes in the Kemp Land region are dominated by a divergent surface-wind field, which would result in the deposition of redistributed surface snow over a wider area down-wind. Without the strong penetration of maritime cyclones across the coastal slopes, the precipitation rate is significantly lower, and net accumulation at a site is largely controlled by interaction between the surface-wind field and snow-redistribution processes. The significant mesoscale topographic roughness in Kemp Land therefore results in the local accumulation-rate pattern being spatially highly variable on the scale of 10 km.

Surface observations and shallow firn drilling (2–5 m deep) in eastern Kemp Land showed extensive depth-hoar formation at elevations of 1850–2700 m on the coastal slopes and on the plateau. This is in strong contrast to other areas on the East Antarctic coastal slopes in Wilkes Land where extensive depth hoar is restricted to the higher elevations of the polar plateau above 2500 m elevation.

The extreme spatial variability of snow accumulation in Kemp Land can best be illustrated along 68°39' S, at an elevation of 1850 m, where sites of extensive depth hoar with very low accumulation rates (less than 20 kg $m^{-2} a^{-1}$ from the 1975–78 cane measurements) exist within 10 km of MGA which has an average accumulation rate of 280 kg $m^{-2} a^{-1}$.

RELATIONSHIP BETWEEN ACCUMULATION AND PASSIVE MICROWAVE EMISSIVITY

The emissivity of dry polar firn at microwave frequencies has typical values in the range 0.65–0.9. Microwave radiation emanating from snow originates from depths of
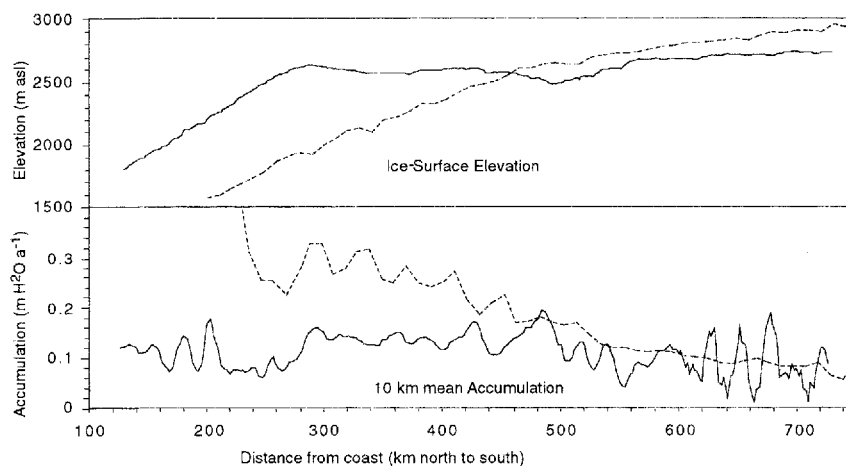

Fig. 2. Comparison of accumulation (10 km means) and elevation profiles for eastern Kemp Land, 60° E (solid lines) and Wilkes Land, 110° E (dashed lines). For eastern Kemp Land, the accumulation measurements from 130 to 610 km are for a 3 year period but only for a 1 year period from 610 to 730 km. Accumulation measurements in Wilkes Land are for a 6 year period.

203

up to several metres below the surface, and the relatively low emissivity is predominantly a result of volume-scattering of the radiation from grains within the snowpack (Zwally, 1977). Larger grains act as more effective volume-scatterers and hence result in a lower emissivity. In snow undergoing destructive metamorphism, grain-size and density increase with time, and the grain-size at any depth is dependent on both the temperature (which determines the rate of metamorphism) and the accumulation rate (which determines the age of the snow at that depth). For horizontally polarized microwave radiation, a secondary contribution to reduced emissivity comes from downward reflection at the snow–air, or an internal, interface which further -decreases outgoing energy. This reflection is related to small-scale surface roughness at the centimetre scale and/ or to the density gradient at the interface (Remy and Minster, 1991). Shuman and others (1993) have shown how formation of surface hoar over an ice sheet can result in a diffuse zone of gradually decreasing density near the surface, with reduced reflection and increased emissivity.

This dependence of microwave emissivity on the physical properties of the snow has been used to derive large-scale estimates of the accumulation-rate distribution over Antarctica from satellite passive-microwave data (e.g. Rotman and others, 1982; Fily and Benoist, 1991). In the region covered by the Lambert Glacier basin traverse, microwave brightness temperature contours as measured by the Nimbus 5 Electronically Scanning Microwave Radiometer (ESMR) are almost orthogonal to elevation contours and must reflect gradients in physical properties other than temperature. Zwally (1977) defined mean emissivity as the ratio of the annual average brightness temperature to the observed mean surface temperature. This has been estimated from annual mean ESMR data for 1976 (19 GHz (1.55 cm), horizontal polarization) and from measured 10 m firn temperatures, which approximate the annual mean surface temperature. Figure 3 shows the mean emissivity and other surface snow properties along the Lambert Glacier basin traverse route (from LGB00 to LGB20 in Figure 1). The values of density, $\delta^{18}O$, crystal diameter (measured with a scale magnifying lens) and number of ice crusts per metre are derived from the mean over the top 2 m of cores taken every 30 km.

On the broad scale, there is a clear correlation between mean microwave emissivity and accumulation rate over the entire 600 km route. Up to about 520 km inland there is also an inverse correlation between emissivity and crystal diameter. The larger grain-sizes are associated with more numerous ice crusts and wind crusts which are produced from wind exposure during an hiatus in accumulation. The minimum in emissivity occurs around the 250 km mark (LGB04, LGB05) where accumulation rates are very low and depth hoar is present, with crystals greater than 1.5 mm in size (compared to near-surface firn-crystal diameters of about 0.7 1.0 mm). North of this, on the coastal slope, accumulation rate, emissivity and crystal size all show strong and parallel gradients, despite high spatial variability in accumulation rates over short distances. The plateau between 300 and 520 km is marked by an
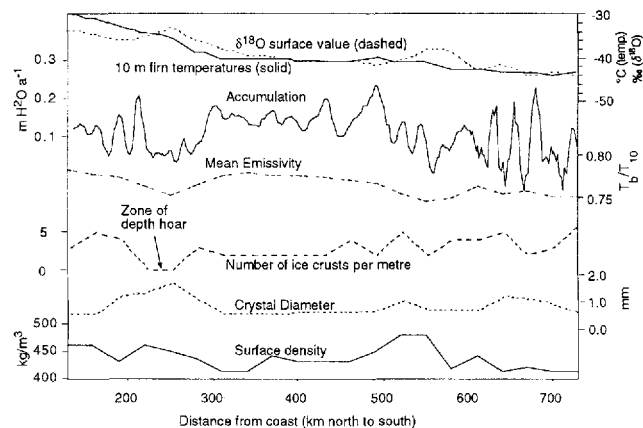

Fig. 3. Profiles of 10 m firn temperature, average $\delta^{18}O$, average accumulation, mean microwave emissivity (19 H) and snow properties along the traverse route between LGB00 and LGB20 (Fig. 1.). Accumulation is shown as 10 km running means. Microwave emissivity (after Zwally, 1977) is derived from annual average ESMR brightness temperatures for 1976 and the measured 10 m firn temperatures. Ice cores were sampled and firn temperatures were measured every 30 km; the $\delta^{18}O$, snow density, crystal diameter and number of ice crusts are averages over the top 2 m.

overall higher and more consistent accumulation regime over short distances, less surface roughness and a slightly smaller crystal diameter; variations in accumulation rate over this zone are well represented in the emissivity. The lower accumulation zone at 500–600 km inland (approximately $100 \, \text{kg m}^{-2} \text{a}^{-1}$) shows as a minimum in emissivity but the crystals remain small. The reduced emissivity in this region may be partly a result of more ice crusts in the firn resulting in greater internal reflection of the upwelling radiation. Further south than 610 km the accumulation rates represent only 1 year, rather than the 3 year average elsewhere, and correlations are less clear.

Microwave brightness temperatures along the western offset route (Fig. 1) are approximately the same or slightly higher than those at an equivalent distance from the coast on the main line. This is despite the fact that the offset elevations are typically 150–200 m higher. Meas-ured accumulation rates are not yet available for this line and it is unclear whether the implied higher emissivity is due to considerably higher accumulation rates along the offset route or to some other effect such as increased surface roughness or lower annual average surface density. Average surface densities for the top 2 m along the offset ranged between 382 and $434 \, \text{kg m}^{-3}$, with a mean of $398 \, \text{kg m}^{-3}$. These were significantly lower than on the main line where the range was 409 471 kg m ^{3} and the mean was $438 \, \text{kg m}^{-3}$. However, shallow-core measurements show there was a tendency for more depth hoar (lower emissivity) to be present on the southern part of the offset line than on the main line. The anomalous gradient in ESMR brightness temperatures in fact extends further westward to the ice divide, which is at over 3000 m elevation.
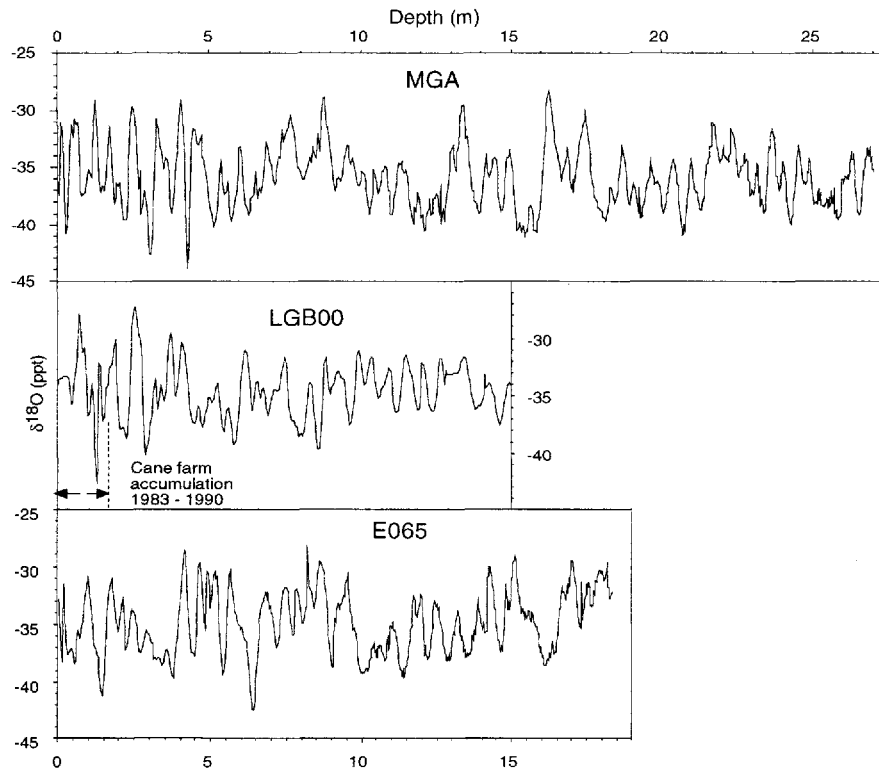
204

Fig. 4. $\delta^{18}O$ profiles from three shallow cores situated within 50 km of each other at 68°39' S. Cores were collected in November 1992 (MGA), February 1991 (LGB00) and February 1993 (E065). Cane measurements from 1975 to 1978 give annual accumulation values at MGA of 0.75 m of snow and at E065 of 0.32 m of snow. Cane-farm measurements from 1983 to 1992 at LGB00 give an annual accumulation of 0.34 m of snow. 7 years of cane-farm accumulation at LGB00 thus corresponds to four apparent $\delta^{18}O$ cycles.

RECENT TEMPORAL VARIABILITY

To determine temporal records of accumulation rate over recent decades, three shallow firn cores were drilled within 50 km of each other approximately along 68°39' S at sites designated LGB00, MGA and E065 (Fig. 1). The sites were selected because they represented the highest known accumulation rates in the 1800–2000 m elevation range in eastern Kemp Land, and depth hoar was not developed at these sites. The accumulation rates measured on canes at each of the sites are 153 (9 year epoch 1983–92), 270 (3 year epoch 1975–78) and 135 kg m^{-2} a^{-1} (3 year epoch 1975–78), respectively. Each of the cores was analysed for visible-layer stratigraphy, oxygen isotope ($\delta^{18}O$) and electrical conductivity. The techniques used were identical to those successfully employed on cores with average accumulation rates of 300–320 kg m^{-2} a^{-1} in Wilkes Land at the same elevation (Goodwin, 1991). The standard model of firn stratigraphy interprets the annual autumn wind-glazed ice crust overlying less-dense firn and a summer radiation-glazed surface as the annual horizon marker (Goodwin, 1991). The autumn wind-glaze ice crust is 0.001–0.005 m thick, opaque and multi-layered, and distinct from the summer radiation glaze, which is less than 0.001 m thick and transparent. Generally, the peak $\delta^{18}O$ signal occurs in snow located above the radiation glaze, whilst the peak conductivity signal occurs in the late summer to early autumn snow, often in association with the autumn wind-glazed ice crust. To account for the relatively low accumulation rates at

LGB00 and E065, the core sampling was conducted using a sampling interval of 3–5 cm or a minimum of eight–ten samples a year.

The $\delta^{18}O$ profiles for the three cores are shown in Figure 4. All three cores show variations in the $\delta^{18}O$ signal that in part seem cyclic. The cyclicity is attributed to the seasonal variation in the $\delta^{18}O$ of precipitation (nominally 8–10‰), but a significant proportion of cycles have an amplitude less than the seasonal variation (e.g. 10.5–12.5 m depth in MGA, 9 15 m depth in LGB00 and 2–4 m depth in E065). The reduced signal amplitude is often due to a lack of isotopically heavier peak summer snowfall (less negative $\delta^{18}O$ values) and to a lesser extent the winter peak values. This would occur if the bulk of the accumulated snow for those years fell during autumn and spring.

Analysis of the $\delta^{18}O$ profiles shows that the wavelength of the cycles corresponds to accumulation rates greater than those measured on the canes. For example, at LGB00 7 years of cane accumulation corresponds to only four $\delta^{18}O$ cycles. Consequently, the observed $\delta^{18}O$ cycles cannot be interpreted as representative of annual accumulation rates. Rather, it is likely that the $\delta^{18}O$ cycles represent the effect of surface-redistribution processes in modifying the accumulation of precipitated and wind-transported snow at a site. At LGB00 and E065, the surface roughness or micro-relief due to snow dunes and sastrugi is approximately equivalent to or greater than 1 year's snow accumulation (0.3 m snow). This region experiences strong katabatic winds and the mean winter wind speed measured at an automatic

205

weather station at LGB00 is in excess of $12\,m\,s^{-1}$ (Allison and others, 1993). Under these conditions, snow is primarily redistributed downwind by saltation and as mobile snow dunes. Strong wind crusts develop over the surface of snow dunes under high winds, which allow their form to be partly preserved in the snowpack. Whilst the $\delta^{18}O$ cycles in the three firn cores resemble seasonal precipitation cycles, it is more appropriate to interpret them as a sample through a mixture of seasonal snow surfaces and stacked snow dunes, i.e. the core intersects a succession of dune morphologies and thicknesses rather than a succession of annual layers. Consequently, the $\delta^{18}O$ cycles represent the stratigraphy and size of the dune which may be maintained above the height of the surrounding snow surface for more than one balance year.

The MGA $\delta^{18}O$ profile shows the most consistent cyclicity of the three cores, indicating that the bulk of precipitation remains in situ rather than being redistributed downwind at this site. However, as is evident in Figure 4 from sections of relative homogeneity in the $\delta^{18}O$ values, there are a number of sections in all the stratigraphic profiles where there appears to be a break or long-term hiatus in the continuous accumulation record. This is supported by a relatively homogeneous conductivity signal and absence of ice crusts and layers. Such homogeneous signals would result from the deposition of a snow dune greater in height than at least 1 year's average accumulation. Thus, accumulation at a site in Kemp Land is likely to be constructed from partial in-situ accumulation of precipitation and to a greater extent from dunes or dune remnants formed from redistributed snow. Accumulation time series could not be derived for the LGB00 and E065 sites, and an accumulation time series from the higher accumulation site at MGA requires independent verification using an absolute-dating horizon (for example, the 1955 or 1965 bomb-radioactivity horizons) to resolve the remaining ambiguities in the core.

CONCLUSIONS

The spatial accumulation pattern in eastern Kemp Land in the elevation range 1850–2700 m is significantly lower than that for the same elevation range in much of East Antarctica. Whilst little is known of the controlling synoptic mechanisms for this precipitation regime, it is apparent that the accumulation at a point is largely a function of the surface-snow redistribution processes and the divergent surface-wind field throughout the western Lambert Glacier basin. The combined stratigraphic investigations of shallow firn cores from relatively low-accumulation areas in a strong katabatic wind zone indicates that it is incorrect to interpret $\delta^{18}O$ cycles as seasonal cycles and to deduce annual accumulation time series from these records. Whilst these stratigraphic methods have been proven to be accurate in high-accumulation areas such as Wilkes Land, where the accumulation rate is $300\,kg\,m^{-2}\,a^{-1}$ or greater, it is apparent from this study that areas with lower accum-

ulation rates are unsuitable for $\delta^{18}O$ stratigraphy. Consequently, it is imperative to have an independent measure of the annual accumulation rate, from either long-term cane measurements or from absolute datable horizons if $\delta^{18}O$ stratigraphy is to be applied to the determination of accumulation-rate time series in low-accumulation areas, which cover much of the interior of East Antarctica.

ACKNOWLEDGEMENTS

REFERENCES

Allison, I., G. Wendler and U. Radok. 1993. Climatology of the East Antarctic ice sheet (100° E to 140° E) derived from automatic weather stations. *J. Geophys. Res.*, **98**(D5), 8815–8823.

Bromwich, D. H. 1988. Snowfall in high southern latitudes. *Rev. Geophys.*, **26**(1), 149–168.

Drewry, D. J. 1983. The surface of the Antarctic ice sheet. *In* Drewry, D. J. *ed. Antarctica: glaciological and geophysical folio.* Cambridge, University of Cambridge. Scott Polar Research Institute, sheet 2.

Drewry, D. J. and E. M. Morris. 1992. The response of large ice sheets to climatic change. *Phil. Trans. R. Soc. Lond.* B338, 235–242.

Fily, M. and J.-P. Benoist. 1991. Large-scale statistical study of Scanning Multichannel Microwave Radiometer (SMMR) data over Antarctica. *J. Glaciol.*, **37**(125), 129–139.

Giovinetto, M. B. and C. Bull. 1987. *Summary and analyses of surface mass balance compilations for Antarctica, 1960–1985.* Byrd Polar Res. Cent., Ohio State Univ., Columbus. (Report 1.)

Giovinetto, M. B., D. H. Bromwich and G. Wendler. 1992. Atmospheric net transport of water vapor and latent heat across 70° S. *J. Geophys. Res.*, **97**(D1), 917–930.

Goodwin, I. D. 1990. Snow accumulation and surface topography in the katabatic zone of eastern Wilkes Land. *Antarct. Sci.*, **2**(3), 235–242.

Goodwin, I. D. 1991. Snow-accumulation variability from seasonal surface observations and firn-core stratigraphy, eastern Wilkes Land, Antarctica. *J. Glaciol.*, **37**(127), 383–387.

Morgan, V. I. and T. H. Jacka. 1979. Mass balance studies in East Antarctica. *In* Allison, I. *ed. Sea Level, Ice and Climatic Change.* International Association of Hydrological Sciences Publication, 131, 253–260.

Remy, F. and J. F. Minster. 1991. A comparison between active and passive microwave measurements of the Antarctic ice sheet and their association with the surface katabatic winds. *J. Glaciol.*, **37**(125), 3–10.

Rotman, S. R., A. D. Fisher and D. H. Staelin. 1982. Inversion for physical characteristics of snow using passive radiometric observations. *J. Glaciol.*, **28**(98), 179–185.

Shuman, C. A., R. B. Alley and S. Anandakrishnan. 1993. Characterization of a hoar-development episode using SSM/I brightness temperatures in the vicinity of the GISP2 site, Greenland. *Ann. Glaciol.*, **17**, 183–188.

Zwally, H. J. 1977. Microwave emissivity and accumulation rate of polar firn. *J. Glaciol.*, **18**(79), 195–215.

The accuracy of references in the text and in this list is the responsibility of the authors, to whom queries should be addressed.